Principles and Practice of Clinical Electrophysiology of Vision

Editors

John R. Heckenlively, M.D.
Professor of Ophthalmology
Jules Stein Eye Institute
Los Angeles, California

Geoffrey B. Arden, M.D., Ph.D.
Professor of Ophthalmology and
Neurophysiology
Institute of Ophthalmology
Moorfields Eye Hospital
London, England

Associate Editors

Emiko Adachi-Usami, M.D.
Professor of Ophthalmology
Chiba University School of Medicine
Chiba, Japan

G.F.A. Harding, Ph.D.
Professor of Neurosciences
Department of Vision Sciences
Aston University
Birmingham, England

Sven Erik Nilsson, M.D., Ph.D.
Professor of Ophthalmology
University of Linköping
Linköping, Sweden

Richard G. Weleber, M.D.
Professor of Ophthalmology
University of Oregon Health Science Center
Portland, Oregon

Mosby Year Book

St. Louis Baltimore Boston Chicago London Philadelphia Sydney Toronto

Mosby
Year Book

Dedicated to Publishing Excellence

Sponsoring Editor: David K. Marshall
Assistant Director, Manuscript Services: Frances M. Perveiler
Production Project Coordinator: Karen E. Halm
Proofroom Manager: Barbara Kelly

A Year Book Medical Publishers imprint of Mosby-Year Book, Inc.

Mosby-Year Book, Inc.
11830 Westline Industrial Drive
St. Louis, MO 63146

1 2 3 4 5 6 7 8 9 0 CL CL MV 95 94 93 92 91

Library of Congress Cataloging-in-Publication Data
Principles and practice of visual electrophysiology / [edited by]
John R. Heckenlively, Geoffrey B. Arden.
p. cm.
Includes bibliographical references.
Includes index.
ISBN 0-8151-4290-0
1. Electroretinography. 2. Electrooculography. 3. Visual evoked response. I. Heckenlively, John R. II. Arden, Geoffrey B. (Geoffrey Bernard)
[DNLM: 1. Electrooculography. 2. Electrophysiology. 3. Electroretinography. 4. Evoked Potentials, Visual. 5. Vision Disorders—physiopathology. WW 270 P957]
RE79.E4P75 1991 91-13378
617.7 1547—dc20 CIP
DNLM/DLC
for Library of Congress

60

Rod and Cone Perimetry: Computerized Testing and Analysis

Samuel G. Jacobson
Peter P. Apáthy
Jean-Marie Parel

The traditional visual function test used to evaluate patients with known or suspected retinal disease is the full-field electroretinogram (ERG). Although the ERG can be exquisitely sensitive to rod- and cone-mediated dysfunction, it cannot provide information about how the dysfunction varies across the retina. The visual field examination can be used to determine regional retinal variations in function, but as performed conventionally, it is not meant to distinguish rod- from cone-mediated dysfunction.

The technique known as "two-color, dark-adapted, static-threshold perimetry" is designed to measure the degree to which rod- and cone-mediated sensitivities are impaired in different retinal regions.[15–17] This test has been applied mainly to the study of patients with retinitis pigmentosa (RP), and results therefrom support the idea that there are subtypes of RP with distinctly different mechanisms of rod and cone dysfunction.[5, 12, 13, 16, 17] Recently, rod and cone perimetric techniques were also used to define patterns of dysfunction in cone-rod dystrophy.[23]

To permit rod and cone perimetry to be performed as part of the routine evaluation of our patients with retinal degeneration, we modified a commercially available computerized perimeter[9] and developed computer programs to analyze and display the data.[1] In this chapter, we review the principles, testing methods, and data analyses for our technique of rod and cone perimetry and provide examples of test results to demonstrate applications of this technology to the understanding of retinal degenerative diseases.

Figure 60–1 illustrates the principles of two-color, dark-adapted, static perimetry. The two curves in each of the four panels are the photopic or cone (dashed lines) and scotopic or rod (solid lines) spectral sensitivity functions.[22] The two wavelengths marked on the curves, 500 nm (circles) and 650 nm (squares), are the two stimulus colors used in this testing. In the fully dark adapted state, with the 500- and 650-nm targets equated in energy, the rod system is about 3 log units (32 dB) more sensitive to the 500-nm than to the 650-nm stimulus, while the cones are 0.8 log units (8 dB) more sensitive to 500 than to 650 nm.

At all extrafoveal test loci in normal subjects, rods mediate detection of both stimuli; this is exemplified in Figure 60–1, upper left. Three types of abnormal visual function are shown in the other panels of Figure 60–1. If both rod and cone sensitivities are impaired to the same degree (Fig 60–1, upper right) or if cone sensitivity is decreased more than that of rods, there will still be rod-mediated detection of the two stimuli. With rod sensitivity impaired more than cone sensitivity there can be "mixed" mediation, i.e., the 500-nm target is detected by the rods, but 650 nm is detected by cones (Fig 60–1, lower left). Cone-mediated detection of both stimuli occurs when there is such severe impairment of rod sensi-

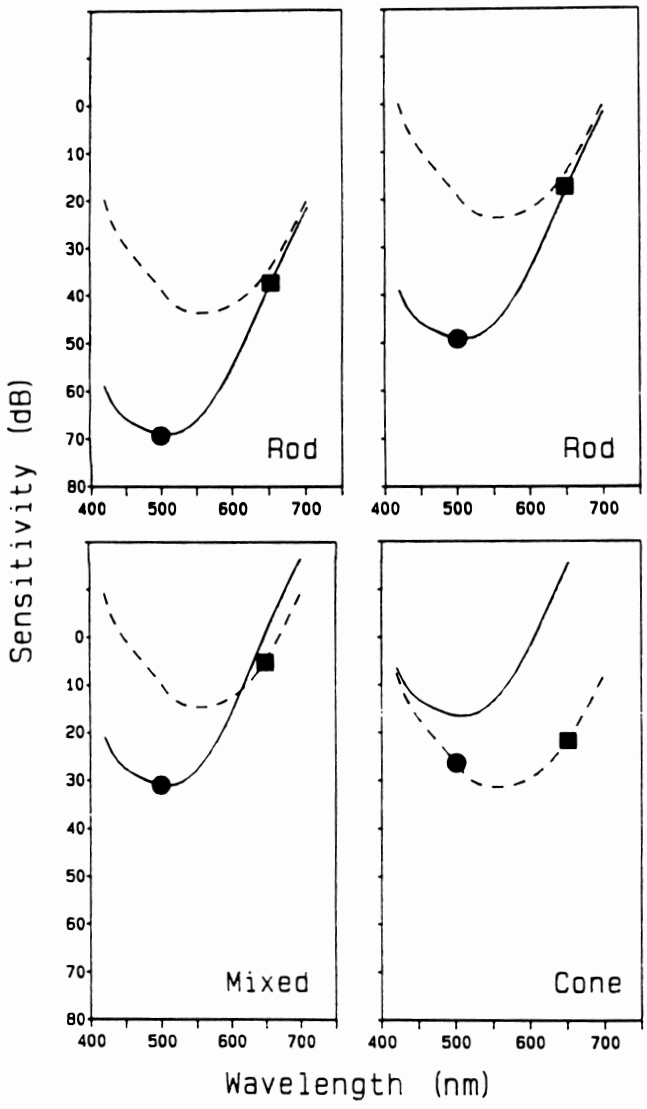

FIG 60–1.
Rod *(solid lines)* and cone *(dashed lines)* spectral sensitivity functions at different positions along the vertical axis relative to one another. The two wavelengths marked on the curves (500 nm, *circles;* 650 nm, *squares*) are those of the test stimuli used in two-color, dark-adapted, static perimetry. Normal rod and cone sensitivity at a locus with rod mediation is in the *upper left,* abnormalities in rod and cone sensitivity with rod mediation are shown in the *upper right,* mixed rod and cone mediation is in the *lower left,* and cone mediation is shown in the *lower right.*

tivity that it is worse than cone sensitivity for both stimulus wavelengths; this can occur in the presence of normal or reduced cone sensitivity (Fig 60–1, lower right).

Thus the difference in sensitivities to the 500- and 650-nm stimuli at a retinal location indicates which photoreceptor mediates detection there. The three possible photoreceptor mediations are (1) rod-mediated detection (sensitivity difference of 32 dB), (2) mixed rod and cone detection (sensitivity difference between 8 and 32 dB), and (3) cone-mediated detection (sensitivity difference of 8 dB). The sensitivity levels, if lower than normal, indicate the degree of sensitivity loss.[1, 9]

As is evident from the upper panels in Figure 60–1, when rods detect both stimuli in the dark-adapted state, there is no measure of cone-mediated sensitivity. For this reason, we also measure sensitivity for a 600-nm target in the light-adapted state (10-cd/m^2 white background light), thereby determining cone-mediated function independent of rod function.

Figure 60–2 is a photograph of the modified computerized projection bowl perimeter; adjacent to it is a microcomputer used for data transfer and analysis. Interference filters were inserted into the optical pathway to be able to test specific stimulus wavelengths, and all stray light leaks into the bowl were eliminated to permit dark-adapted thresholds to be measured. An infrared television system was installed for monitoring of fixation in the light and dark. A full-field test strategy was devised to examine 75 loci (on a 12-degree grid with 4 extra loci centrally) and a foveal locus within an elliptical field of vision extending 72 degrees temporally, 48 degrees nasally, 36 degrees superiorly, and 48 degrees inferiorly. Details of these and other modifications have been published.[9]

The test session begins with instruction of the patient about the purpose and conduct of the proce-

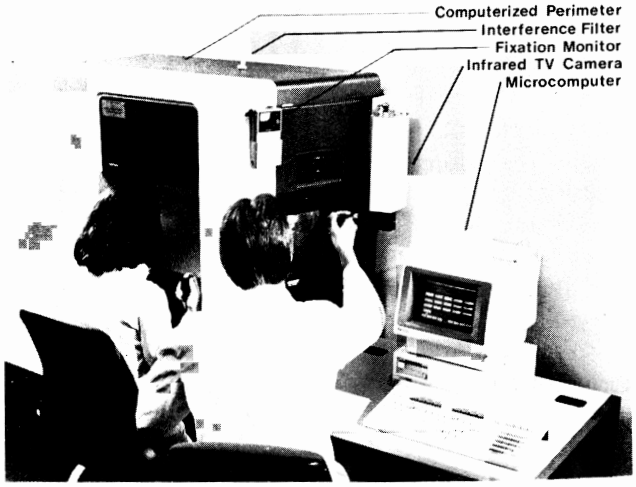

FIG 60–2.
Instrumentation used to perform and to analyze data from rod and cone perimetry.

dure. To familiarize the patient with the testing, provide practice at the test, and determine the locations of any absolute scotomas, a rapid "screening" test is administered first.[3] This test is performed monocularly by using the full-field test strategy (75 loci) in the light-adapted state with a white stimulus target (Goldmann size V, 103-minute diameter; single intensity of 3,183 cd/m^2) and requires no more than 3 to 4 minutes per eye for completion. If the results from the two eyes are symmetrical, only one eye is tested thereafter. After mydriatic-cycloplegic eyedrops are instilled and have taken effect in the test eye, threshold testing is performed first in the light-adapted state (600-nm target, 103-minute diameter). The patient's test eye is then dark-adapted (45 minutes), and the threshold protocol is repeated in the dark-adapted state for the 650-nm and 500-nm targets (103-minute diameter). The test time for each full-field threshold test is about 15 minutes. The fixation pattern of the patient is determined at each test session by using either a visuscope or a fundus perimeter; if fixation is not central, the position of the eccentric fixation locus is noted so that the results of the perimetry can be interpreted correctly.[23] Patients with high refractive errors wear corrective soft contact lenses during the test.

Figure 60–3 shows the steps in the analyses of the light-adapted thresholds and the two sets of dark-adapted threshold measurements. The automated perimeter is used only to collect and store the raw data; all further analyses are performed on an auxiliary microcomputer. Software has been developed to determine photoreceptor mediation from the results of the dark-adapted testing; statistical cri-

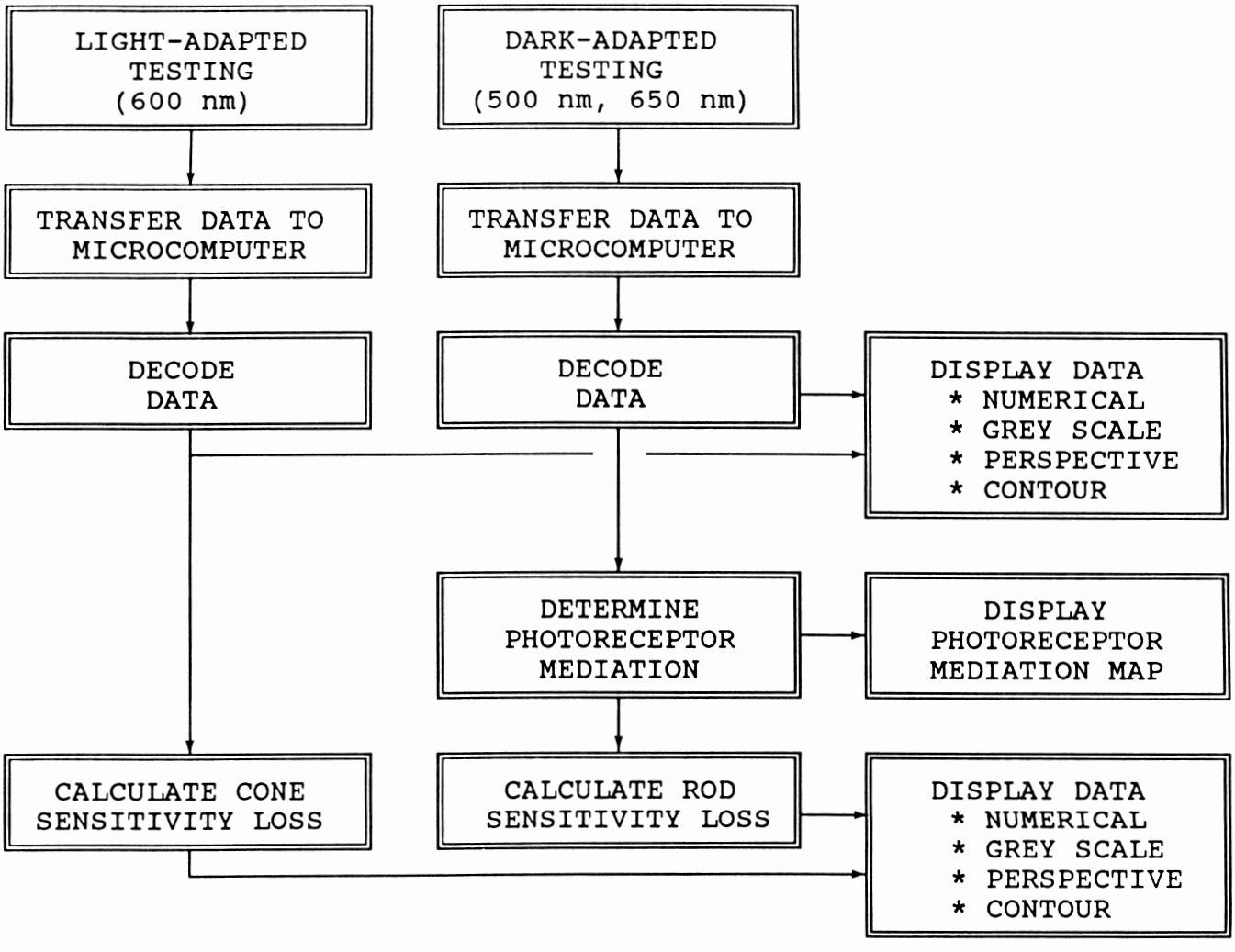

FIG 60–3.
Steps in the processing of data from rod and cone perimetry.

teria are used to classify test loci as rod, cone, or mixed.[1] Rod sensitivity loss is determined for rod and mixed loci by comparing the patient's dark-adapted sensitivity at 500 nm to that of the normal mean sensitivity for each locus. Cone sensitivity loss is based on comparisons between the patient and normal mean light-adapted sensitivity to 600 nm. Sensitivity loss is only calculated for test loci with abnormal sensitivity (defined as lower than 2.6 SD from the normal mean at the locus).

Figure 60–4 shows the results of rod and cone perimetry in the left eyes of two patients with typical RP.[6, 14] These results exemplify the two different types of visual dysfunction identified in autosomal dominant and simplex/multiplex RP.[12, 13, 16, 17] In the upper row are the photoreceptor mediations at

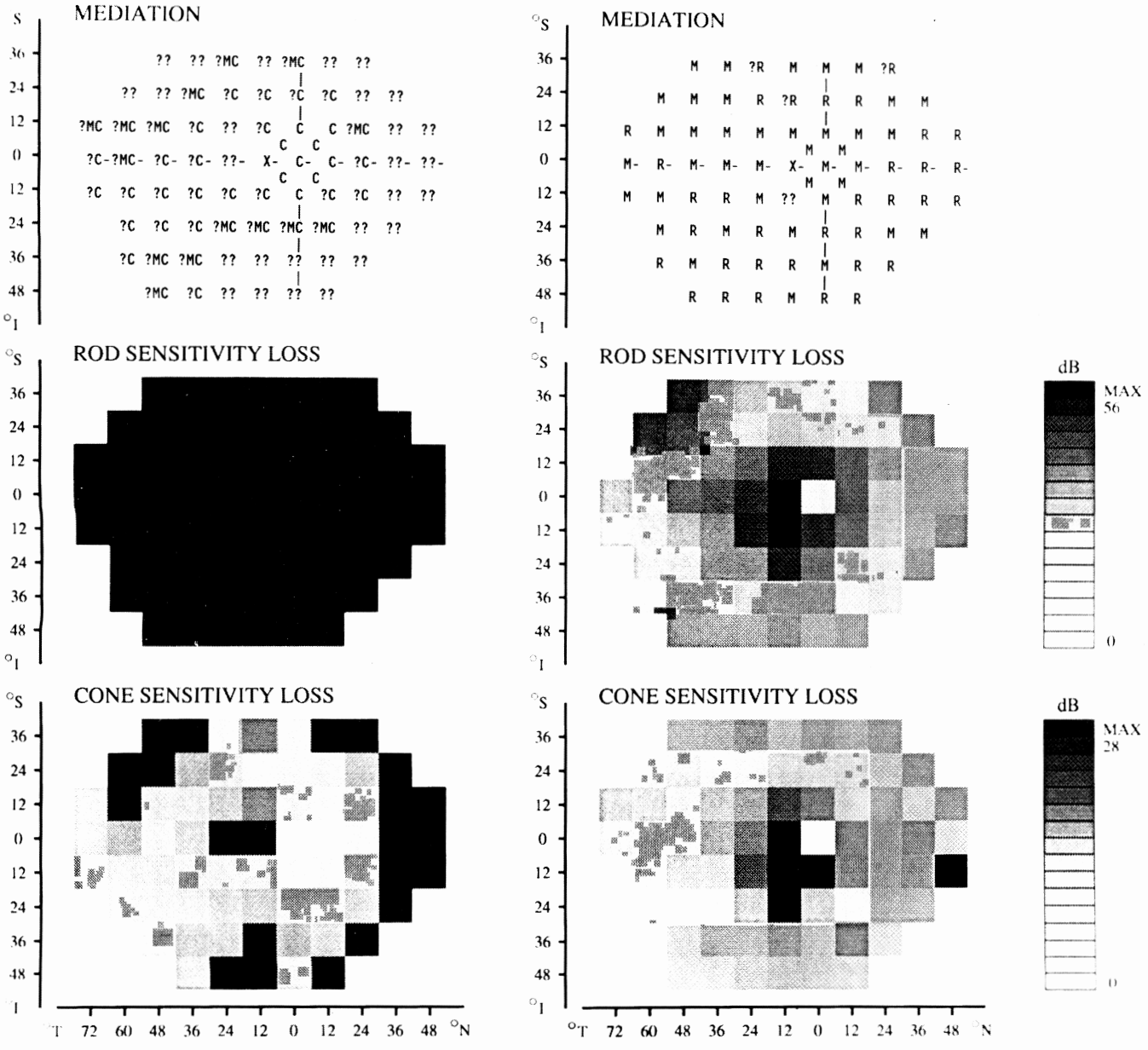

FIG 60–4.
Photoreceptor mediation at each of the 75 test locations *(upper row)* and rod *(middle row)* and cone *(lower row)* sensitivity losses displayed in gray scale for the left eyes of two patients with RP *(left* and *right columns)* representing different functional subtypes. Gray scale representation employs 15 levels of gray, each covering a 4-dB range in sensitivity loss. Maximum *(MAX)* loss is shown as black. See the text for an explanation of symbols in the mediation map.

each of the 75 test loci based on the results of two-color, dark-adapted, static perimetry. The symbols R, M, and C represent rod, mixed and cone mediation; where a question mark precedes these mediations, only one color was detected.[1] Double question marks indicate that neither color was detected and mediation was therefore impossible to determine from the data; "X" is the blind spot. In the middle row are gray scale maps of rod sensitivity loss, and in the lower row are the maps of cone sensitivity loss. Black indicates that there was no measurable response at the locus to the maximum-intensity stimulus. Rod sensitivity loss at cone-mediated loci is indeterminate and also displayed as black.

The data in the left column of Figure 60–4 are from a 24-year-old man with simplex RP, i.e., having no known affected relatives[14]; there was no detectable rod ERG, and the cone signal was reduced in amplitude and delayed in implicit time. The mediation map shows cone-mediated detection at all loci where there were measurable responses to both colors. Rod sensitivity loss is profound, and the effect is diffuse across the visual field. Cone sensitivity is abnormal except at certain central field loci; in the nasal field and several other peripheral locations, the patient did not detect the 600-nm target. This pattern of visual dysfunction has been termed "type 1"[16, 17] or "diffuse"[5, 12, 13] RP.

The data in the right column of Figure 60–4 are from a 48-year-old woman, also with simplex RP; her rod ERGs were moderately reduced in amplitude and delayed in implicit time, while the cone ERGs showed minimal amplitude reductions with delayed timing. The mediation maps indicate rod- and mixed-mediated detection throughout the field. Both rod and cone sensitivity are measurable in most of the visual field, but there is regional variation in severity. The pericentral and midperipheral regions show greater rod and cone sensitivity losses than elsewhere in the field. This pattern of visual dysfunction has been termed "type 2" or "regionalized" RP.

Figure 60–5 shows rod and cone perimetric results from the left eyes of two patients with cone-rod dystrophy (CRD). Both patients have more rod than cone function with the ERG but show very different distributions of function across their visual fields. These patients' perimetric results exemplify two of the three recently defined patterns of visual dysfunction in CRD.[23] In the left column of Figure 60–5 are data from a 28-year-old woman with autosomal recessive CRD; her rod ERGs were moderately reduced in amplitude and delayed in timing, and the cone ERGs showed severe amplitude reductions with delayed timing. Like many patients with CRD, this patient has eccentric fixation; the maps have been shifted by the angle of eccentricity to permit a comparison with normal data. Unmeasured regions of the nasal field (due to the eccentric fixation) are labeled "U" on the mediation map and displayed as scotomatous in the gray scale maps. The mediation map indicates mainly rod but also a few mixed loci. The gray scales show a central rod and cone scotoma, some midperipheral rod and cone function, peripheral rod function, but little or no measurable peripheral cone function.

The data in the right column of Figure 60–5 are from a 21-year-old man, also with autosomal recessive CRD, who has central but slightly unsteady fixation; his rod ERG was markedly reduced, and there was no detectable cone ERG. Like the other CRD patient, most measurable loci are rod mediated, but the regional variation in sensitivity across the visual field differs from that in the other patient. There is some rod function in a large central island separated from small islands in the inferotemporal peripheral field by a midperipheral scotoma. There is no measurable cone sensitivity throughout the visual field (to 600 nm on a background; but there is one M locus).

Figure 60–6 shows results of rod and cone perimetry from both eyes of a 48-year-old woman who is a heterozygote (carrier) of X-linked retinitis pigmentosa (XLRP). In this retinopathy, there is a wide spectrum of disease expression from minimal or none to severe, and unlike other forms of RP, the heterozygous state of XLRP can show significant interocular asymmetries in visual function.[11] The rod and cone ERGs in the right eye of this patient showed slightly lower than normal amplitudes and timing delays; in the left eye amplitudes fell within the normal range, but there was a delay in cone flicker timing. Mediation in the left eye (Fig 60–6, left column) is mainly rod but with a few mixed loci; the right eye (Fig 60–6, right column) shows many more mixed loci than the left. The gray scales show patches of rod and cone dysfunction in both eyes; the severity of dysfunction, however, is greater in the right eye than in the left eye, and the locations of the dysfunctional areas are not the same in the two eyes. Different relationships of rod-to-cone dysfunction have been found in recent rod and cone perimetry studies of XLRP heterozygotes and hemizygotes.[7, 8, 10, 21] Such phenotypic differences may be of considerable interest since there is increasing evidence for different genotypes within XLRP.[2, 4, 18–20]

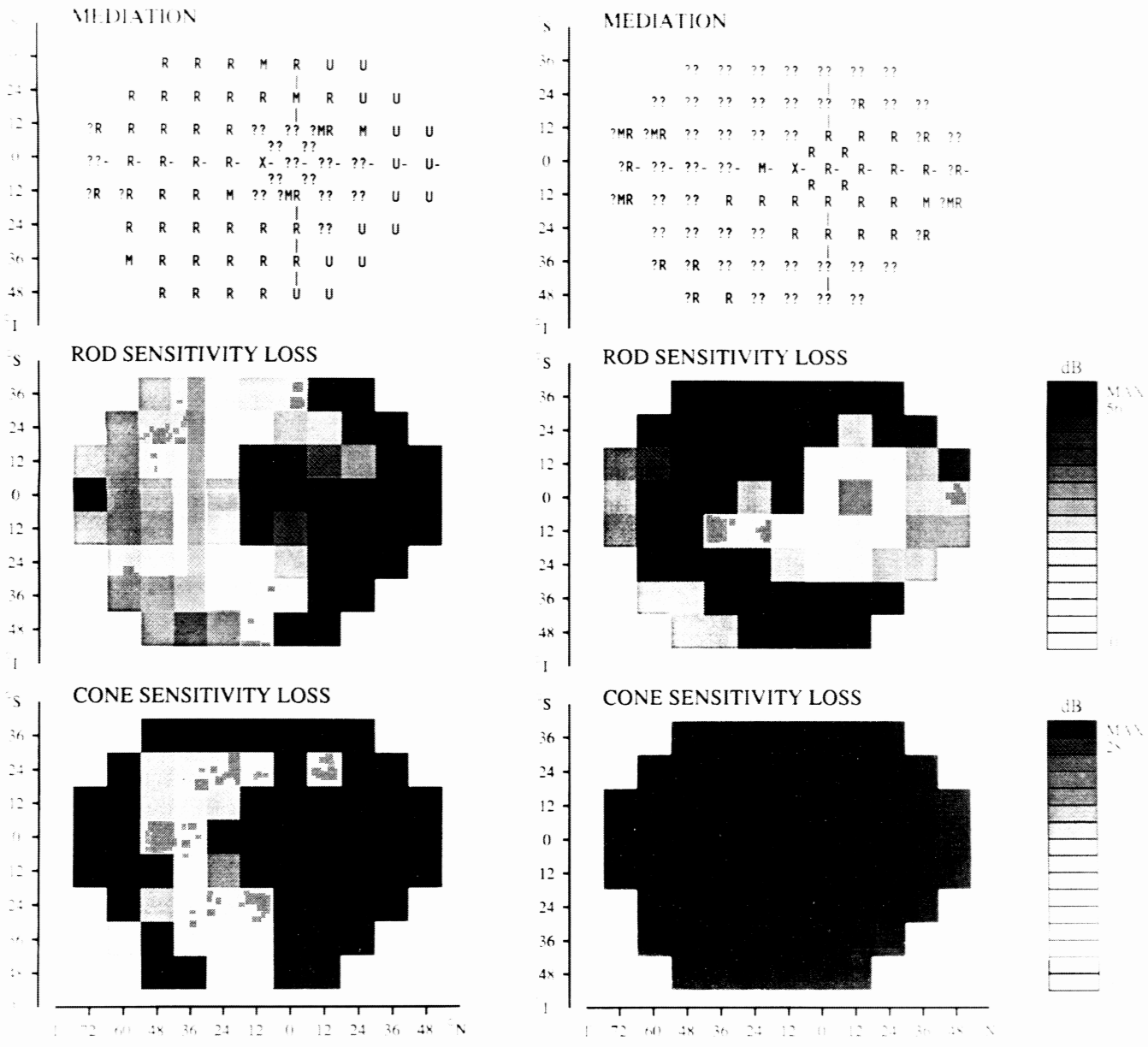

FIG 60–5.
Photoreceptor mediations and rod and cone sensitivity loss maps for the left eyes of two CRD patients with different patterns of dysfunction.

In conclusion, rod and cone sensitivity measurements throughout the visual field provide information about regional retinal variations in rod and cone dysfunction that is not available from other more routine electrophysiological and psychophysical tests of visual function. With this information, two functional subtypes of RP and three patterns of dysfunction in CRD have been identified. Although relatively time-consuming, computerized rod and cone perimetry has become part of our routine evaluation of patients with retinal degenerations. The test results not only help to identify functional subcategories of retinal diseases but also provide clinically useful information about the degree of day and night vision disturbances suffered by these patients. Such information often helps to explain the patients' symptoms and affords an accurate basis for giving them counsel about their visual disabilities.

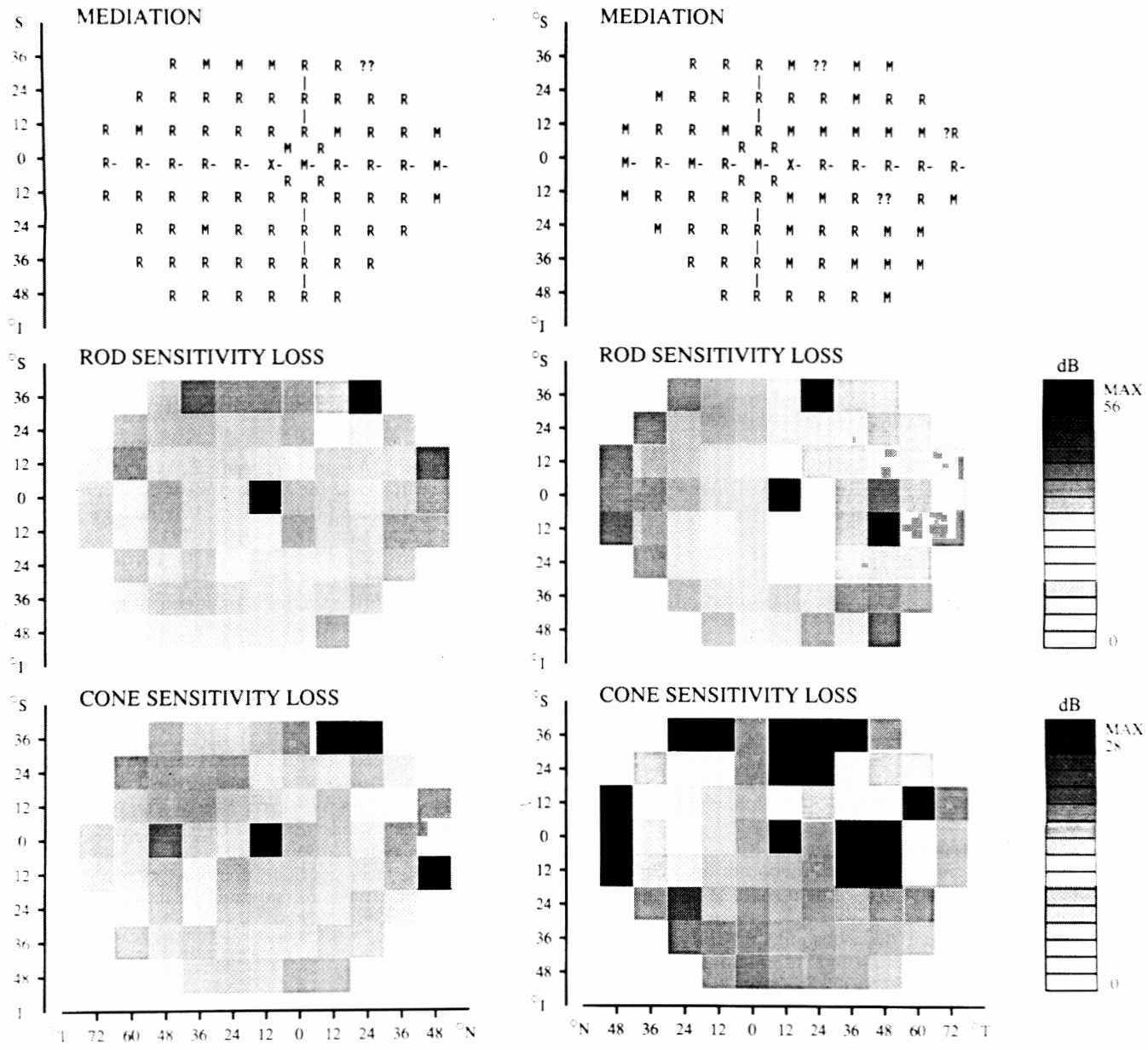

FIG 60–6.
Photoreceptor mediations and rod and cone sensitivity loss maps for the right and left eyes of a heterozygote of XLRP.

Acknowledgments

We thank the National Retinitis Pigmentosa Foundation, Inc. (Baltimore), and The Chatlos Foundation, Inc. (Longwood, Fla), for support. We are also grateful to Drs. Robert Knighton, Karla Batlle, and Katsuya Yagasaki for critical advice and help; Drs. Steve Myers, Lan Nghiem-Phu, and Marisa Roman for development of computer programs; and Barbara French for artwork.

REFERENCES

1. Apáthy PP, Jacobson SG, Nghiem-Phu L, Knighton RW, Parel JM: Computer-aided analysis in automated dark-adapted static perimetry, in Greve EL, Heijl A (eds): *Seventh International Visual Field Symposium*, Dordrecht, The Netherlands, Martinus Nijhoff Publishers, 1987, pp 277–284.
2. Bhattacharya SS, Wright AF, Clayton JF, Price WH, Phillips CI, McKeown CME, Jay M, Bird AC, Pearson PL, Southern EM, Evans J: Close genetic linkage be-

tween X-linked retinitis pigmentosa and a restriction fragment length polymorphism identified by recombinant DNA probe L1.28. *Nature* 1984; 309:253–255.
3. Borruat F-X, Jacobson SG: Advanced retinitis pigmentosa: Quantifying visual function, in Hollyfield JG, Anderson RE, LaVail MM (eds): *Inherited and Enviromentally Induced Retinal Degenerations.* New York, Alan R Liss, Inc, 1989, pp 3–17.
4. Denton MJ, Chen J-D, Serravalle S, Colley P, Halliday FB, Donald J: Analysis of linkage relationships of X-linked retinitis pigmentosa with the following X_p loci: L1.28, OTC, 754, XJ-1.1, pERT87, and C7. *Hum Genet* 1988; 78:60–64.
5. Ernst W, Faulkner DJ, Hogg CR, Powell DJ, Arden GB, Vaegan: An automated static perimeter/ adaptometer using light emitting diodes. *Br J Ophthalmol* 1983; 67:431–442.
6. Heckenlively JR: The diagnosis and classification of retinitis pigmentosa, in Heckenlively JR (ed): *Retinitis Pigmentosa.* Philadelphia, JB Lippincott, 1988, pp 6–10.
7. Jacobson SG, Apáthy PP, Yagasaki K, Feuer WJ, Batlle K, Roman MI, Roman AJ: Cone-rod dysfunction in X-linked retinitis pigmentosa. *Invest Ophthalmol Vis Sci* 1989; 30(suppl):45.
8. Jacobson SG, Chiu MT, Yagasaki K, Apathy PP: Cone and rod dysfunction in carriers of X-linked retinitis pigmentosa. *Invest Ophthalmol Vis Sci* 1987; 28(suppl):112.
9. Jacobson SG, Voigt WJ, Parel JM, Apathy PP, Rausch NH: Automated light- and dark-adapted perimetry for evaluating retinitis pigmentosa. *Ophthalmology* 1986; 93:1604–1611.
10. Jacobson SG, Yagasaki K, Chiu MT, et al: X-linked retinitis pigmentosa: Retinal function abnormalities in heterozygotes and hemizygotes. *J Cell Biochem* 1988; 12B(suppl):237.
11. Jacobson SG, Yagasaki K, Feuer WJ, Roman AJ: Interocular asymmetry of visual function in heterozygotes of X-linked retinitis pigmentosa. *Exp Eye Res* 1989; 48:679–691.
12. Kemp CM, Faulkner DJ, Jacobson SG: Two types of visual dysfunction in autosomal dominant retinitis pigmentosa. *Invest Ophthal Vis Sci* 1988; 29:1235–1241.
13. Lyness AL, Ernst W, Quinlan MP, Clover GM, Arden GB, Carter RM, Bird AC, Parker JA: A clinical, psychophysical and electroretinographic survey of patients with autosomal dominant retinitis pigmentosa. *Br J Ophthalmol* 1985; 69:326–339.
14. Marmor MF: Retinitis pigmentosa: A symposium on terminology and methods of examination. *Ophthalmology* 1983; 90:126–131.
15. Massof RW: Psychophysical subclassifications of retinitis pigmentosa, in LaVail M, Hollyfield JG, Anderson RE (eds): *Retinal Degeneration: Experimental and Clinical Studies.* New York, Alan R Liss, Inc, 1985, pp 91–107.
16. Massof RW, Finkelstein D: Rod sensitivity relative to cone sensitivity in retinitis pigmentosa. *Invest Ophthalmol Vis Sci* 1979; 18:263–272.
17. Massof RW, Finkelstein D: Two forms of autosomal dominant primary retinitis pigmentosa. *Doc Ophthalmol* 1981; 51:289–346.
18. Mussarella MA, Burghes A, Anson-Cartwright L, Mahtani MM, Argonza R, Tsui LC, Worton R: Localization of the gene for X-linked recessive type of retinitis pigmentosa (XLRP) to Xp21 by linkage analysis. *Am J Hum Genet* 1988; 43:484–494.
19. Nussbaum RL, Lewis RA, Lesko JG, Ferrell R: Mapping ophthalmological disease. II. Linkage of relationship of X-linked retinitis pigmentosa to X-chromosome short arm markers. *Hum Genet* 1985; 70:45–50.
20. Oh J: Localizing multiple X chromosome-linked retinitis pigmentosa loci using multilocus homogeneity tests. *Proc Natl Acad Sci USA* 1990; 87:701–704.
21. Peachey NS, Fishman GA, Derlacki DJ, Alexander KR: Rod and cone dysfunction in carriers of X-linked retinitis pigmentosa. *Ophthalmology* 1988; 95:677–685.
22. Wyszecki G, Stiles WS: *Color Science: Concepts and Methods, Quantitative Data and Formulae*, ed 2. New York, John Wiley & Sons, Inc, 1982.
23. Yagasaki K, Jacobson SG: Cone-rod dystrophy: Phenotypic diversity by retinal function testing. *Arch Ophthalmol* 1989; 107:701–708.